Available online at www.sciencedirect.com
ScienceDirect
Biochimica et Biophysica Acta 1767 (2007) 22–30
Biochimica et Biophysica Acta
BBA
www.elsevier.com/locate/bbabio

Energy and electron transfer in the photosynthetic reaction center complex of *Acidiphilium rubrum* containing Zn-bacteriochlorophyll *a* studied by femtosecond up-conversion spectroscopy

Tetsuo Tomi [a], Yutaka Shibata [a], Yuki Ikeda [a], Seiji Taniguchi [b], Chosrowjan Haik [b], Noboru Mataga [b], Keizo Shimada [c], Shigeru Itoh [a,*]

[a] *Department of Material Science (Physics), Graduate School of Science, Nagoya University, Furocho, Chikusa, Nagoya 464-8602, Japan*
[b] *Institute for Laser Technology, Utsubo-Hommachi 1-8-4, Nishi-ku, Osaka 550-0004, Japan*
[c] *Department of Biology, Graduate School of Science, Tokyo Metropolitan University, Minamiohsawa 1-1, Hachioji, Tokyo 192-0397, Japan*

Received 27 June 2006; received in revised form 11 October 2006; accepted 27 October 2006
Available online 1 November 2006

Abstract

A photosynthetic reaction center (RC) complex was isolated from a purple bacterium, *Acidiphilium rubrum*. The RC contains bacteriochlorophyll *a* containing Zn as a central metal (Zn-BChl *a*) and bacteriopheophytin *a* (BPhe *a*) but no Mg-BChl *a*. The absorption peaks of the Zn-BChl *a* dimer (P_{Zn}), the accessory Zn-BChl *a* (B_{Zn}), and BPhe *a* (H) at 4 K in the RC showed peaks at 875, 792, and 753 nm, respectively. These peaks were shorter than the corresponding peaks in *Rhodobacter sphaeroides* RC that has Mg-BChl *a*. The kinetics of fluorescence from P^*_{Zn}, measured by fluorescence up-conversion, showed the rise and the major decay with time constants of 0.16 and 3.3 ps, respectively. The former represents the energy transfer from B^*_{Zn} to P_{Zn}, and the latter, the electron transfer from P_{Zn} to H. The angle between the transition dipoles of B_{Zn} and P_{Zn} was estimated to be 36° based on the fluorescence anisotropy. The time constants and the angle are almost equal to those in the *Rb. sphaeroides* RC. The high efficiency of *A. rubrum* RC seems to be enabled by the chemical property of Zn-BChl *a* and by the L168HE modification of the RC protein that modifies P_{Zn}.

Keywords: Electron transfer; Energy transfer; Fluorescence up-conversion; Purple photosynthetic bacteria; Reaction center; Zn-bacteriochlorophyll *a*

1. Introduction

Until the discovery of an acidophilic purple photosynthetic bacterium, *Acidiphilium rubrum* (*A. rubrum*), it had been believed that only Mg-containing pigments, chlorophylls (Chls) and bacteriochlorophylls (BChls) are used in natural photosynthesis [1]. *A. rubrum* has a pigment like BChl *a* that contains Zn as a central metal (Zn-bacteriopheophytin *a* according to the chemical nomenclature) as the major pigment with a small percentage of Mg-BChl *a*. We call this natural Zn-containing pigment here Zn-bacteriochlorophyll *a* (Zn-BChl *a*) according to a proposal by Takaichi et al. [2]. *A. rubrum* contains Zn-BChl *a* [1,3–5]. We isolated the reaction center (RC) complex from this organism and studied the function mechanism of Zn-BChl *a*-based photosynthesis by up-conversion spectroscopy.

A. rubrum is an acidophilic aerobic proteobacterium that grows at pH 1.5–7.5 (even in the dark) [1,3,5–9], produces Zn-BChl *a* [7] without specific addition of Zn, and accumulates heavy metals like Fe, Cr, Ni too [10–12]. The organism has a light-harvesting core antenna (LH1) complex and an RC complex that contains Zn-BChl *a* almost exclusively [1,4,5], together with bacteriopheophytin *a,* spirilloxanthins, and ubiquinone [4,5,13,14]. Other *Acidiphilium* species also contain Zn-BChl *a*, but in smaller amounts [4,5,13,14]. The biosynthetic pathway of Zn-BChl *a* in *A. rubrum* produces Mg-protoporphyrin IX monomethyl ester at first, and then, Mg is

Abbreviations: BChl *a*, bacteriochlorophyll *a*; BPhe *a*, bacteriopheophytin *a*; B_{Zn}, accessory Zn-BChl *a*; Chl *a*, chlorophyll *a*; P_{Zn}, special pair of Zn-BChl *a*; RC, reaction center

* Corresponding author. Tel.: +81 52 789 2883; fax: +81 52 789 2883.
E-mail address: itoh@bio.phys.nagoya-u.ac.jp (S. Itoh).

0005-2728/$ - see front matter © 2006 Elsevier B.V. All rights reserved.
doi:10.1016/j.bbabio.2006.10.008

replaced by Zn by an unknown mechanism [5,7,15]. The other organisms like *Chlorella* are also known to accumulate Zn-Chl *a* partially, however, after forced adaptation to a Zn-abundant growth condition [16].

The atomic weight of Zn (MW 65.41) is twice that of Mg (MW 24.31), however, Zn^{2+} and Mg^{2+} have similar ionic radii of 0.88 and 0.86 Å, respectively. Mg-BChl *a* and Zn-BChl *a*, thus, have similar but a little different molecular features. Mg-BChls have 5- and 6-coordinated Mg^{2+} [17] and only 5-coordinated ones were found in photosynthetic proteins, while synthesized Zn-porphyrins are known to adopt only 4- or 5-coordinated states [18,19]. Zn-BChl *a* shows optical and redox properties similar to those of Mg-BChl *a* [20,21]. The fluorescence lifetime of Zn-Chl *a* (9.0 ns) is comparable to that of Mg-Chl *a* (9.8 ns) in a micellar solution [22]. Zn-porphyrin derivatives that are more stable than Mg-derivatives [20,22] have been frequently used in attempts of artificial photosynthesis [23,24]. Mg-BChl *a* easily loses Mg below pH 4, while Zn-BChl *a* loses Zn only below pH 1 [4,25]. These features of Zn-BChl *a* suggest it to be also useful in photosynthesis. However, the natural photosynthesis with Zn-BChl *a* has only been found in *Acidiphilium* species.

The absorption spectrum of the isolated RC complex of *A. rubrum* resembles that of other purple bacterial RCs [3,5]. Zn-BChl *a* molecules function as the special pair (P) and as the two accessory pigments (B) in the RC. We designate P and B of *A. rubrum* as P_{Zn} and B_{Zn}, respectively, hereafter in this paper to avoid confusion. The absorption peaks at 875 and 792 nm of P_{Zn} and B_{Zn}, respectively, are blue-shifted by 10–20 nm compared to the peaks of P and B (made of Mg-BChl *a*) in the other purple bacterial RCs. A magnetic circular dichroism (MCD) measurement of *A. rubrum* RC suggested the monomeric nature of oxidized P_{Zn} ($=P^{+}_{Zn}$) and the circular dichroism (CD) spectra suggested a weaker interaction between the two Zn-BChls of P_{Zn} compared to that between the two Mg-BChls of P in the other bacteria [26].

The amino acid sequences, especially of those interacting with the chromophores, of the light (L), medium (M), and heavy (H) subunits of the RC and α and β subunits of LH1 in *A. rubrum* are well conserved to their counterparts in other purple bacteria [27]. However, the 168th histidine in the L subunit protein (L168H), which is located nearby P and is conserved in purple bacterial RCs, is glutamate in *A. rubrum*. The substitution was suggested to compensate for the physicochemical features of P_{Zn} that are different from those of P made of Mg-BChl *a* [27].

In purple bacterial photosynthesis, light energy absorbed by antenna pigments is funneled into P [28–30], and the excited special pair (P*) transfers an electron within 3 ps to H (BPhe *a*) on the L subunit [31,32]. B and H also rapidly transfer excitation energy to P. The angle between the transition dipoles of B and P was measured to be 32° in the RC of *Rhodobacter sphaeroides* by the measurement of fs-time resolved fluorescence anisotropy [33], in agreement with the structure revealed by X-ray crystallography [34]. In this study, we measured the energy transfer and electron transfer times as well as this angle to know the structure and function of the RC with Zn-BChl *a*.

We isolated the RC complex from *A. rubrum* and measured the fs-fluorescence dynamics by using a fluorescence up-conversion method to know the excitation energy transfer process from B^{*}_{Zn} to P_{Zn} and the electron transfer process from P_{Zn} to H_L. The results demonstrate the efficient energy and electron transfer processes in the Zn-BChl *a* containing RC.

2. Materials and methods

2.1. Culture of A. rubrum cells and isolation of the RC complex

A. rubrum cells were grown in a growth medium at 30 °C in the dark at pH 3.5 according to Shimada et al. [3]. Membranes and RC complexes of *A. rubrum* were prepared by treatment with a detergent, LDAO (N-N-Lauryldimethylamine N-oxide), followed by ultracentrifugations and column chromatography [3]. The RC complex of *Rb. sphaeroides* was prepared according to a method reported previously [35] with some modifications [36].

2.2. Measurement of the absorption spectrum at low temperature

The RC complex, which had been dissolved in a 20 mM phosphate buffer (pH 7.8), was placed in a plastic cuvette with a 1 cm path length. Glycerol was added to the reaction mixture to give a final concentration of 66% (v/v). The sample with reduced P_{Zn} (reduced with 2 mM sodium ascorbate) or oxidized P_{Zn} (oxidized with 1 mM potassium ferricyanide) was then cooled down to cryogenic temperatures in a liquid helium cryostat (Oxford Inst., Oxford). A UV-3100PC UV-VIS-NIR spectrophotometer (Shimadzu, Kyoto) was used to measure the absorption spectra.

2.3. Measurement of femto-second time-resolved fluorescence up-conversion

The RC complex, which had been dissolved in a 10 mM phosphate buffer (pH 7.8) and 2 mM sodium ascorbate, was placed in a quartz cuvette with a 2 mm optical path length and stirred by a magnetic stirrer during the experiment. The optical density of the sample at 790 nm was adjusted at 0.4. The set-up of the fluorescence up-conversion was described elsewhere [37]. The excitation laser pulse was generated by a Ti:Sapphire laser (Coherent MIRA). The laser pulse had a spectral width of 10 nm fwhm (full width at half maximum) and a half duration of 110 fs and was given at a repetition rate of 80 MHz. The laser pulse at 815 nm was separated into two beams; the one excited the sample directly and the other was collected to BBO crystal after passing through an optical delay stage. The fluorescence (947 nm) emitted from the sample was also collected to the same BBO crystal and the two light were transformed to an up-conversion light (438 nm) by sum-frequency conversion. The intensity of the up-conversion light was measured with varying the delay between the excitation and gate pulses to measure the time dependence of the sample fluorescence. Polarization of the fluorescence was measured by changing the angle of the half-wave plate inserted in the excitation path. The anisotropy $R(t)=(I(t)_{\parallel}-I(t)_{\perp})/(I(t)_{\parallel}+2I(t)_{\perp})$ in a ps-time region was calculated. Here, $I(t)_{\parallel}$ and $I(t)_{\perp}$ represent the fluorescence intensities at time t detected at parallel and perpendicular polarization angles, respectively, with respect to the polarization of the excitation beam.

2.4. Redox titration of P in A. rubrum membranes

Anaerobic titration of the redox midpoint potential (E_m) value of P_{Zn} in *A. rubrum* membranes was carried out under nitrogen gas in an airtight cuvette as described elsewhere [38]. The oxidation of P_{Zn} upon excitation by a 10 ns, 532 nm flash from an Nd-YAG laser (Spectra Physics, LAB-130) was monitored as the absorbance change at 810 nm. The sample cuvette contained membranes that were suspended in a 20 mM Tris–HCl buffer (pH 7.5) to give a final concentration of 1.5 OD at 861 nm. The following redox mediators were added at 1–20 μM: 1,2-naphthoquinone, 1,4-naphthoquinone, duroquinone, 2-hydroxy-1,4-naphthoquinone, methylene blue, and 2,3,5,6-tetramethyl-*p*-

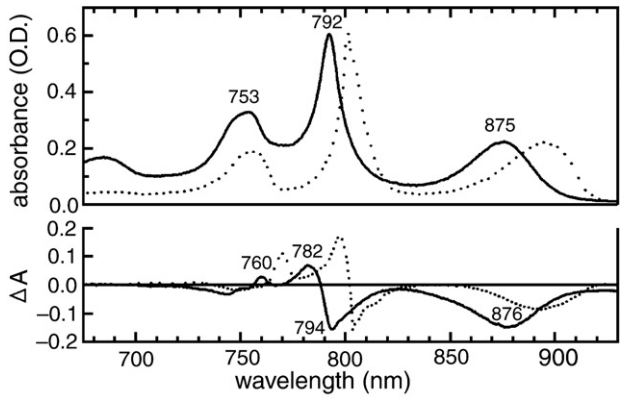

Fig. 1. Upper panel: Absorption spectrum of the *A. rubrum* RC at 4 K (solid line) and the *Rb. sphaeroides* RC at 6 K (dotted line). Lower panel: Oxidized-minus-reduced difference spectrum of the *A. rubrum* RC (solid line) at 4 K and the *Rb. sphaeroides* RC (dotted line) at 10 K. The spectra of the *Rb. sphaeroides* RC were reproduced from Franken et al. [39].

phenylene diamine. Potassium ferricyanide, potassium ferrocyanide, sodium ascorbate and sodium dithionite dissolved in water at 0.001–1 mM were also used as required. The obtained titration data were fitted by a Nernst equation with $n=1$ to calculate the E_m value.

3. Results

3.1. Absorption and difference absorption spectra of RC complex of A. rubrum containing Zn-BChl a

The upper panel in Fig. 1 shows the absorption spectrum of the *A. rubrum* RC at 4 K (solid lines) together with that of the *Rb. sphaeroides* RC at 6 K (dotted lines), which was reproduced from Franken et al. [39]. The spectrum of the *A. rubrum* RC resembles that of the *Rb. sphaeroides* RC, which is one of the best characterized RCs. The peak wavelengths of the absorption bands became longer at the lower temperature. The peak wavelength of P_{Zn} (special pair of Zn-BChl *a*) shifted to the red more significantly than the peaks of B_{Zn} (accessory Zn-BChl *a*) and H (BPhe *a*) band on cooling. The Q_y bands of P_{Zn} and B_{Zn} were blue-shifted by 10 and 20 nm, respectively, compared to those of *Rb. sphaeroides*, as expected from the fact that they were made of Zn-BChl *a*, as reported previously [3,5]. The peak position of the H band in the *A. rubrum* RC showed a small 6 nm difference even though BPhe *a* does not contain Zn. The energy levels of P and B or their excited state levels were calculated from the absorption spectra of the RC complex of *Rb. sphaeroides* at 293 K [40] and *A. rubrum* at 277 K [26] as shown in Table 1.

Table 1
Energy levels in *Rb. sphaeroides* and *A. rubrum* RC. P_+ and P_- are the higher and lower levels of the two excitonically split states of P, respectively

RC	P_+ (eV)	P_- (eV)	B (eV)	H (eV)	Reference
Rb. sphaeroides (293 K)	1.521	1.425	1.544	1.632	[40]
A. rubrum (277 K)	1.539	1.468	1.566	1.654	[26]

Table 2
Comparison of the peak positions of the absorption spectra of the *A. rubrum* RC with those of *Rb. sphaeroides*

RC	P (nm)	B (nm)	H (nm)	Reference
Rb. sphaeroides (6 K)	895	802	759	[39]
Rb. sphaeroides (295 K)	865	802	760	[32]
A. rubrum (4 K)	875	792	753	This work
A. rubrum (284 K)	859	792	754	This work and [3]

The oxidized-minus-reduced difference spectrum of the *A. rubrum* RC (solid line) at 4 K is also shown in the lower panel together with that of the *Rb. sphaeroides* RC (dotted line) measured at 10 K [39]. The difference spectrum of the *A. rubrum* RC shows positive peaks at 760 and 782 nm and negative ones at 794 and 876 nm. The peak at 760 nm can be assigned to be the red shift of the Q_y peak of the H band. The band position was slightly different from that of *Rb. sphaeroides*. The negative peak at 876 nm is produced by the oxidation of P_{Zn} and sharp changes at 782–794 nm can be assigned to the electrochromic shift of B_{Zn} in response to the oxidation of P_{Zn}. These peaks are significantly blue-shifted compared to those in the *Rb. sphaeroides* RC.

The absorption maxima of RC cofactor bands at various temperatures are given in Table 2. These values give the features of P_{Zn}, B_{Zn}, and H in the RC.

3.2. Excitation energy transfer and electron transfer within the A. rubrum RC

The up-converted fluorescence was measured at 438 nm as the sum frequency of emission of P^*_{Zn} (947 nm) and the gate beam (815 nm). Fig. 2 shows the time courses of the fluorescence from P^*_{Zn} in the *A. rubrum* RC (triangles in the upper panel) and P^* in the *Rb. sphaeroides* RC (circles in the lower panel) measured at 947 nm at a magic angle with respect to the 815 nm excitation pulse, respectively, measured as the intensities of up-conversion fluorescence at room temperature. The excitation pulse mainly excited B. The fluorescence at

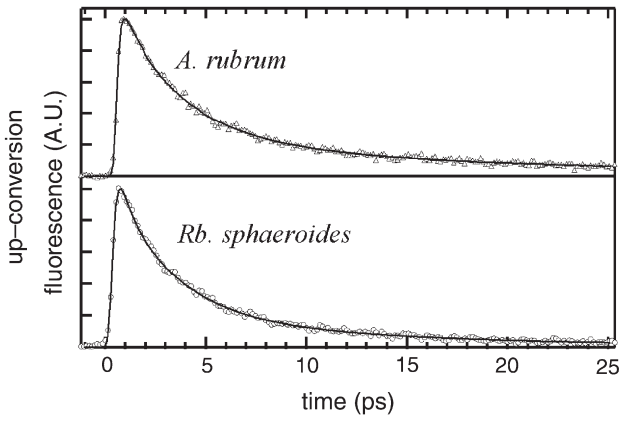

Fig. 2. Time courses of the fluorescence measured at 947 nm in RC complexes of *Rb. sphaeroides* (circles) and *A. rubrum* (triangles) excited at 815 nm. Solid lines are fitting curves made of 4 exponential functions convoluted with the IRF (instrument response function).

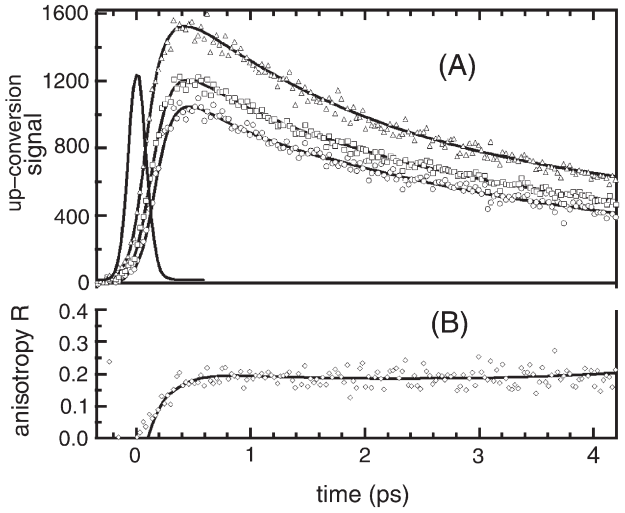

Fig. 3. Dependence of the fluorescence kinetics on the detection-polarized angles with respect to the polarization of the excitation laser beam at room temperature. Upper panel: fluorescence time courses at 947 nm detected at parallel (triangle), magic (square), and perpendicular (circle) angles to the excitation laser polarization in the *A. rubrum* RC complex excited at 815 nm. The solid lines show the fitting curves. A curve with a peak at 0 ps represents the IRF. Lower panel: fluorescence anisotropy $R(t)$. The solid line shows $R(t)$ calculated using the fitting curves in the upper panel. See text for details.

around 947 nm was emitted from P^* which was produced after the energy transfer from B. The rise and decay of the fluorescence in both RCs resembled each other, suggesting the fast energy transfer and charge separation.

The fluorescence time courses of P^*_{Zn} were also measured in the faster time scales at parallel, perpendicular, and magic polarization angles with respect to the excitation beam as shown in Fig. 3. A Gaussian shape peak at time zero shows the instrumental response function (IRF) evaluated from the laser time profile. The rise time of the fluorescence is longer than the width of IRF; therefore, the rise and decay time constants could be precisely estimated. Solid lines are the fitting curves calculated as a sum of 4 exponential functions with different time constants, in which one component with a negative amplitude represents the rise.

The fluorescence time course of P^*_{Zn} at a magic angle was well fitted with a rise time of 0.16 ps and decay components with lifetimes of 0.40 ps (34%), 3.3 ps (53%), and 16 ps (13%). The fluorescence time course in the *Rb. sphaeroides* RC was also fitted with a rise time of 0.16 ps and decay constants of 0.27 ps (48%), 3.0 ps (46%), and 20 ps (6%). These values in the *Rb. sphaeroides* RC are in good agreement with those estimated in previous studies [30,32]. The time constant of the rise of P^*_{Zn} was 0.16 ps and was almost similar to that of P^* measured in the *Rb. sphaeroides* RC here or previously [32,41]. In the fluorescence decay profile of P^*_{Zn}, the fast 0.40 ps phase was smaller in extent than that with the time constant of 0.27 ps in *Rb. sphaeroides*. The contribution of the slow 16 ps component of P^*_{Zn} was larger than the corresponding 20 ps component in the *Rb. sphaeroides* RC. The fitting parameters used for the decays are given in Table 3.

Table 4
Anisotropy and angles between P and B calculated from the fluorescence decay

RC	Anisotropy	Angle between P and B
Rb. sphaeroides	0.24	32°
A. rubrum	0.19	36°

3.3. Depolarization of the fluorescence

The upper panel in Fig. 3 shows the fluorescence time courses monitored at 947 nm at two polarization angles with respect to the excitation laser at 815 nm at room temperature in the *A. rubrum* RC. The rise detected at the parallel angle was faster than that at the perpendicular angle. The lower panel in Fig. 3 shows the calculated anisotropy $R=(I_{\parallel}-I_{\perp})/(I_{\parallel}+2I_{\perp})$. The anisotropy value attained a constant level of 0.19 at 1–4 ps after the rise with a 0.16 ps time constant that indicates the energy transfer time from B_{Zn} to P_{Zn}. From the R-value of 0.19, we estimated an angle of 36° between the transition dipole moments of the photoexcited molecule (presumably B_{Zn} and a part of P_{Zn+}) and the emitting molecule (P^*_{Zn}). The angle of 36° calculated is close to that (32°) obtained in fluorescence anisotropy measurements in the *Rb. sphaeroides* RC by Stanley et al. [33] and King et al. [41]. The anisotropy values calculated from the fluorescence decay in the *Rb. sphaeroides* and *A. rubrum* RCs are given in Table 4.

3.4. Redox potential of P_{Zn}

We performed the redox titration of P_{Zn} in isolated membranes of *A. rubrum* (Fig. 4). A redox midpoint potential value of P_{Zn}/P^+_{Zn} was determined to be +440 mV, similar to the E_m value of 440–450 mV of P/P^+ measured in chromatophore membranes of *Rb. sphaeroides* [42,43].

In the purified RC of *Rb. sphaeroides*, the measured midpoint potential of P was approximately 500 mV, slightly higher than that in the membrane [32,44–47]. It has been assumed that the redox potential of a special pair becomes more positive due to the change in the interaction between the special pair and the surrounding RC proteins by the extraction of the RC [47]. The E_m value of P_{Zn} in the purified RC of *A. rubrum*, thus, is likely to be slightly higher than that in the membrane. We tried to titrate the E_m of P_{Zn} in the purified RC of *A. rubrum*

Table 3
Fitting parameter for the fs-time courses of fluorescence decay measured in Fig. 2

RC	Amp1 (%)	τ_1 (ps)	Amp2 (%)	τ_2 (ps)	Amp3 (%)	τ_3 (ps)	τ rise (ps)
Rb. sphaeroides	48	0.27	46	3.0	6	20	0.16
A. rubrum	34	0.40	53	3.3	13	16	0.16

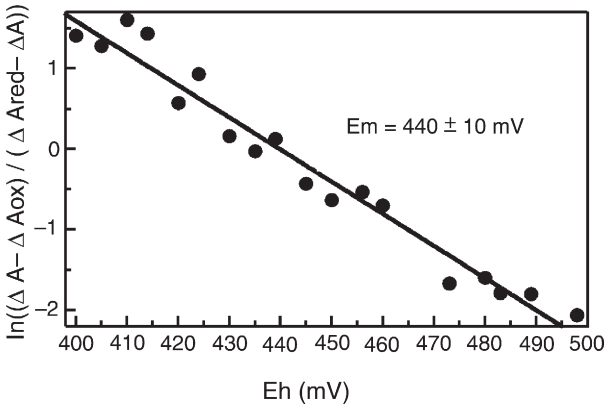

Fig. 4. Redox titration of P_{Zn} (Zn-BChl *a* dimer) in isolated membranes of *A. rubrum* at pH 7.5. Titration was done as described in Materials and methods. The data points were fitted by a Nernst equation with $n=1$ to calculate the E_m value.

but failed to obtain a reliable value because of the aggregation of the RC complex during the titration.

4. Discussion

4.1. Comparison of the RCs of A. rubrum and Rb. sphaeroides

The isolated RC complex of *A. rubrum* contains Zn-BChl *a* in the place of Mg-BChl *a* as the special pair P_{Zn} and the accessory pigments B_{Zn}. The other components, such as the electron acceptors BPhe *a* and ubiquinones, are the same as those in other purple bacterial RCs [5]. The amino acid sequences of the polypeptides of L, M, H, and C subunits show high homologies, except for a few residues that will be discussed later, to those in other purple bacterial RCs that bind tetraheme cytochrome *c*, such as *Rhodopseudomonas viridis* [27]. The C subunit and ubiquinone are depleted in the LDAO-derived RC used in the present study [3]. The structure of the *A. rubrum* RC, thus, is assumed to be quite similar to those of other purple bacterial RCs except for the use of Zn-BChl *a*. The absorption spectrum of the *A. rubrum* RC at 4 K revealed a feature expected for purple bacterial RCs, namely, peak wavelengths of B_{Zn} and P_{Zn} at similar but slightly shorter wavelengths than P and B in the *Rb. sphaeroides* RC, as expected for Zn-BChl *a*. The peak of H also shifted to the blue slightly due to the unknown reason. It is also noted that the oscillator strength estimated from the absorption band of P_{Zn} at 850 nm is somewhat smaller than that of P in the *Rb. sphaeroides* RC, suggesting weaker interaction between the Zn-BChl *a* molecules forming P_{Zn}, as has been indicated [26].

The redox potentials of P_{Zn} and P in the membranes of *A. rubrum* and *Rb. sphaeroides* are 440 and 450 mV, respectively (Fig. 5) so that if we expect similar relation, as well as similar redox potentials of H in the two types of isolated RCs, the energy level of P^+H^- state will be almost equal each other (with a difference of about 10 mV). The shorter peak wavelength suggests the energy level of P^*_{Zn} in *A. rubrum* RC to be about 20 meV higher than that of P^* in *Rb. sphaeroides*. As a result, the energy gap between the P^* and P^+H^- states should be larger for *A. rubrum* by around 30 mV than for *Rb. sphaeroides*. The free energy gap ($-\Delta G$) between P^* and P^+H^- in *Rb. sphaeroides* has been estimated to be 120–260 mV, though it might vary depending on the time scale [44,48–52].

The results in the present study indicate that the energy transfer rate from B_{Zn} to P_{Zn} as well as the electron transfer rate from P_{Zn} to H in *A. rubrum* is almost equal to the corresponding ones in the *Rb. sphaeroides* RC. The results may either come from the similar values of energy gaps or from some other reasons that are specific for Zn-BChl *a* as discussed below.

4.2. Redox potential of P in the A. rubrum RC

The redox titration of P_{Zn} in *A. rubrum* membranes gave the midpoint potential of +440 mV (Fig. 4), similar to that of P at 440–450 mV determined in the chromatophore membranes of other purple bacteria [42,43]. Although the E_m value of P_{Zn} in the RC preparation of *A. rubrum* was not determined, the value is likely to be similar or slightly more positive than that in the membranes, as known for many purple bacterial RCs [42,43,45]. In most purple bacterial RCs, the E_m of P has been measured to be around 500 mV [32,44–47].

The similarity of the E_m value of P_{Zn} to that of P in *Rb. sphaeroides* RC, may be as expected because the E_m values of Mg-BChl *a* and Zn-BChl *a* are similar at around +600 mV (NHE) in organic media [20,53,54]. On the other hand, in the *Rb. sphaeroides* RC, in which a portion of the special pair Mg-BChl *a* was replaced by Zn-BChl *a* artificially [55], the E_m of artificially-produced P_{Zn}, which was formed in the 30% of RC, was 520 mV. The value was 36 mV more positive than that of the remaining portion of P, which are made of Mg-BChl *a* [55]. This 36 mV positive shift of E_m is a little larger than the observed 10 mV negative shift of E_m in P_{Zn} of the *A. rubrum* membrane compared to that of P in the *Rb. sphaeroides* membrane. The difference might be related either to the different RC conditions or to the different protein structure as discussed below.

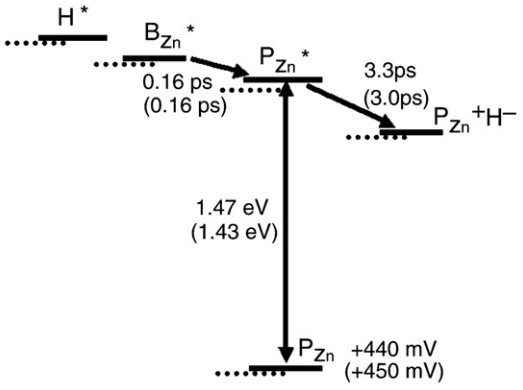

Fig. 5. Energy diagrams of the components in the *A. rubrum* RC assuming that the level of P^*_{Zn} (Zn-BChl *a*) is the same that of P^* (Mg-BChl *a*). The rates of energy transfer and electron transfer in *A. rubrum* RC are shown. Broken lines and values in parenthesis represent the corresponding ones measured in *Rb. sphaeroides* RC, respectively.

4.3. Excitation energy transfer within the RC

The fluorescence of P^*_{Zn} in the *A. rubrum* RC showed a fast rise time of 160 fs upon the excitation of B_{Zn} at 815 nm. The time constant was almost identical to energy transfer time from B^* to P measured in the *Rb. sphaeroides* RC in this study or as listed below; a decay time constant of 160 fs was obtained by monitoring the B^* fluorescence at 850 nm upon the excitation of B at 804.5 nm at 85 K [41]; the rise time of 163 fs of the emission from P^* at 940 nm was detected upon the excitation of B at 804 nm [33]; the rise time of 85±17 fs (H^* to B) and the decay time of 199 fs (B^* to P) were also reported for B^* measured at 815 nm upon the excitation of the H band at 760 nm at 85 K [41]. These 160–199 fs time constants are almost identical to the 160 fs one measured in the *A. rubrum* RC. It is, therefore, concluded that the energy transfer time from B^*_{Zn} to P_{Zn} in the *A. rubrum* RC is quite similar to the corresponding ones in other RCs.

Theoretical analysis indicated that the energy transfer from B to P occurs through the P_+ state, which is the higher level of the excitonically split two states of P at around 810 nm [56]. The B^*_{Zn} to P_{Zn} energy transfer rate in the *A. rubrum* RC suggests a similar extent of the overlap of the P_{Zn+} and B^*_{Zn} bands to that of the P_+ and B^* reported in the RC of *Rb. sphaeroides*. It might be enabled by the blue shifts of both P_{Zn} and B_{Zn} bands. The rate of the energy transfer from H, which showed a smaller blue shift compared to those of P_{Zn} and B_{Zn}, to B_{Zn} in *A. rubrum* is interesting though it remains to be studied.

The energy difference between the P_{Zn+} and P_{Zn-} states has been estimated to be 570 cm^{-1} in the *A. rubrum* RC, smaller than the corresponding 900 cm^{-1} in the *Rb. sphaeroides* RC, on the basis of the absorption, CD, and MCD spectra [26]. The low-temperature absorption spectra in Fig. 1 support this conclusion. The lower energy difference suggests a weaker interaction between the two Zn-BChls of P_{Zn} in *A. rubrum* than that between the two Mg-BChls of P in *Rb. sphaeroides* [26]. In the quinone-depleted *Rb. sphaeroides* R-26 RC, a 200 fs lifetime of fluorescence, which was detected with the excitation at 608 nm, was concluded to be contributed by the internal conversion rate from P_+ to P_- [57]. A similar situation seems to be expected for *A. rubrum*.

In the *A. rubrum* RC, we did not observe the oscillation of the fluorescence of P^*_{Zn} upon the excitation of B. It is similar to the observation by Stanley et al. [33] who reported that the fluorescence from P^* did not oscillate when B was selectively excited in the *Rb. sphaeroides* RC.

The very fast decay time (0.40 ps) of P^*_{Zn} (τ_1) detected in the *A. rubrum* RC was also similar to that detected in the *Rb. sphaeroides* RC (0.27 ps). The mechanism for this component is still unclear, but may represent the early electron transfer from P to H. The 16 ps decay time of P^*_{Zn} (τ_3) detected in the *A. rubrum* RC was also almost equal to that detected in the *Rb. sphaeroides* RC that was depleted of Q_A, although the mechanism for this decay component is not clear yet [57].

We can conclude that the rates of energy transfer and electron transfer in the *A. rubrum* RC are very similar to those in the *Rb. sphaeroides* RC in spite of the weaker interaction between Zn-BChls of P_{Zn} and the extensive blue shift of the peak wavelength of P_{Zn}.

4.4. Angle between P and B

The anisotropy of the fluorescence measured upon the excitation of the B_{Zn} band at 815 nm and the detection of the P_{Zn} emission at 947 nm gave a 0.19 value of polarization at room temperature at 1–4 ps and a mutual angle of 36° between the transition dipoles of B_{Zn} and P_{Zn}. The angle is comparable to that of 32° obtained in the *Rb. sphaeroides* RC upon the excitation at 804.5 nm at 85 K [41]. Although the derived value is not the exact one between the transition dipoles of B and P because of the mixture of P_+ and $B_\pm$ at 815 nm [56], it agrees well with the one revealed by X-ray crystallography [34]. It is, therefore, suggested that *A. rubrum* has the RC that has a structure very similar to that of *Rb. sphaeroides*.

4.5. Electron transfer rates in A. rubrum

Among the decay components of fluorescence from P^*_{Zn}, the one with a time constant of 3.3 ps (τ_2) can be estimated to represent the major process in the initial charge separation (P^*_{Zn} to $P^+_{Zn}H^-$). The time constant is almost identical to that measured in the *Rb. sphaeroides* RC. Thus, the difference of the central metal does not seem to have a substantial effect on the primary charge separation rate.

In the framework of Marcus's electron transfer theory, the electron transfer rate should show a bell-shaped dependence on the free energy gap $-\Delta G$ of the reaction [58]. Haffa et al. [59] showed a sharp bell-shaped dependence of the initial charge separation rate with a peak of $-\Delta G$ at 130 meV in the *Rb. sphaeroides* RC by modifying the redox midpoint potential of P by site-directed mutagenesis. A small change of $-\Delta G$ from the naturally optimized value resulted in the slower rate of primary charge separation [58]. We detected a charge separation rate of 3.3 ps in the *A. rubrum* RC that was identical to that in *Rb. sphaeroides* wild type RC. It may, therefore, suggest that a slight change in the $-\Delta G$ value between the P^*_{Zn} and $P^+_{Zn}H^-$ levels in the *A. rubrum* RC from that in the *Rb. sphaeroides* does not strongly affect the electron transfer rate although the energy level of blue-shifted P^*_{Zn} is expected to be a little higher than that of P^* due to the shorter wavelength peak position.

4.6. Effect of protein

The amino acid sequences of the RC polypeptides of *A. rubrum* have high homologies to those of purple bacterial RCs [27]. It has been noted that the highly conserved residue L168H nearby P is not histidine, and is glutamate in *A. rubrum*. The substitution was suggested to modify the properties of P_{Zn} [5]. We considered this effects below. Fig. 6 shows the absorption spectra at room temperature of various RC preparations that were isolated from (a) *A. rubrum* in this work, (b) wild type and (c) L168HE mutant strains of *Rb. sphaeroides* [59] and (d) RC of *Rb. sphaeroides* in which P, but not of B, are chemically exchanged to Zn-BChl *a* [55]. The spectrum (d) was obtained

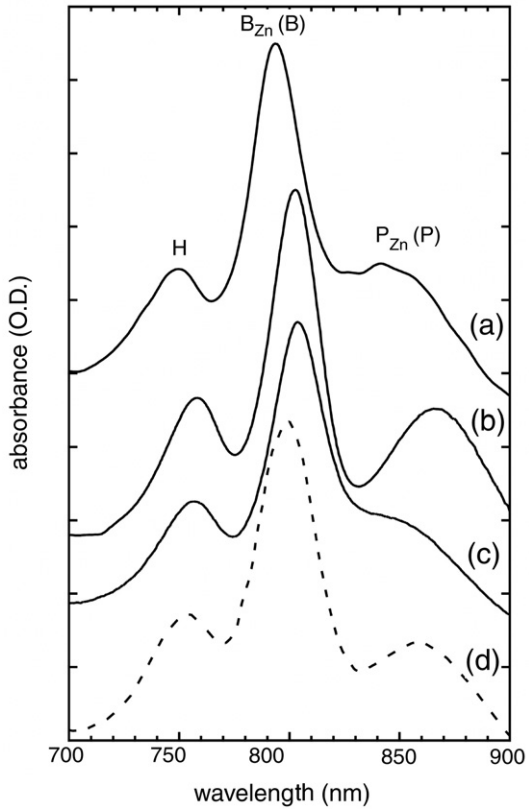

Fig. 6. Absorption spectrum of the purified RC of (a) *A. rubrum*, (b) *Rb. sphaeroides* wild type, (c) *Rb. sphaeroides* L168HE mutant strain, and (d) *Rb. sphaeroides* RC in which Mg-BChl *a* molecules of P (P_{Zn}), but not of B, are chemically exchanged to Zn-BChl *a*. All the spectra were measured at room temperature. The spectra of (c) and (d) were reproduced from Haffa et al. [59] and Kobayashi et al. [55], respectively.

after the subtraction of the co-existing RC spectrum that still contains Mg-BChl *a* because of the low 30% yield of the pigment exchange in the presence of detergent [55].

A. rubrum RC showed a spectrum (a) with blue-shifted peaks of B_{Zn} and P_{Zn} compared to those of B and P in a spectrum (b) of wild type *Rb. sphaeroides* RC as confirmed in Fig. 1. The blue shifts can be ascribed to Zn-BChl *a*. The spectrum, however, is somewhat different from the spectrum (d). The low peak height of P_{Zn} in spectrum (a) suggests the weaker electronic coupling between Zn-BChl *a* molecules of P_{Zn} [26]. However, the spectrum (d) shows a rather high peak of artificially-formed P_{Zn} with the smaller extent of blue shift. B that is a monomer of Mg-BChl *a* in spectrum (d) does not show the blue shift as expected.

The spectrum (c) represents the RC of an L168HE mutant of *Rb. sphaeroides* that has a glutamate at L168 position in the place of histidine in wild type RC and contains Mg-BChl *a* both for P and B [59]. The mutant RC showed an E_m of P at 428 mV, which was more negative than that of wild type, and a fast 2.1 ps decay time of P* [59]. The P peak is shifted to 847 nm (giving an up-shift of 20 mV in the transition energy compared to the 861 nm P peak in the wild type spectrum (b)). The free energy gap for the initial electron transfer, thus, was up-shifted by 99 mV compared to the wild type [59]. The spectral features of P in spectrum (c) with a peak at a short wavelength and with the lower peak height resemble those of P_{Zn} in *A. rubrum* in the spectrum (a). It is, therefore, suggested that the L168HE modification gives rather strong effects on the spectral feature of P_{Zn} too in *A. rubrum* RC.

We can conclude that the replacement of Mg to Zn of central metal of BChl *a* contributes to the blue shifts of B_{Zn} and P_{Zn} bands in the *A. rubrum* RC. H bands were slightly affected too by the replacement. It is also likely that the significant blue shift and the lower peak height of P_{Zn} in *A. rubrum* RC are produced through the effect of L168E residue. This modification, at the same time, seems to work to shift the E_m of P_{Zn} to be more negative as seen for P in the mutant RC [59]. Without this modification, the E_m of P_{Zn} might have been more positive because the artificially-formed P_{Zn} in *Rb. sphaeroides* RC gave a 36 mV positive shift of E_m [55]. Altogether E_m of P_{Zn} in *A. rubrum* gives a value almost similar to that of P in *Rb. sphaeroides* wild type RC. The conservations of this specific residue in multiple *Acidiphilium* strains [27] also seem to support this idea. It is interesting that the deviation from the optimum $-\Delta G$ setting for the charge separation reaction induced by the introduction of Zn-BChl *a* into the special pair (P_{Zn}) seems to be almost compensated by the L168HE modification. The effects of the replacement of B to B_{Zn} or of the shift of H band remains to be studied.

5. Conclusion

The rates of primary electron transfer and energy transfer in the *A. rubrum* RC that contains Zn-BChl *a* as B_{Zn} and P_{Zn} were almost the same as those in the RC of *Rb. sphaeroides* that contains Mg-BChl *a*. The RC with Zn-BChl *a* is shown to be a fully efficient photosynthetic system. The results in the present study suggest that it is enabled by the physicochemical property of Zn-BChl *a*, which resembles that of Mg-BChl *a*, and probably by the L168HE modification of RC protein to adjust the redox potential of P_{Zn}. It remains to be studied whether this mechanism works well even in intact cells of *A. rubrum*, in which P_{Zn}-side of the RC complex in the cytoplasm membrane faces to the outer acidic medium. The reason why Zn-BChl *a* has not been used in the other photosynthetic systems still remains to be studied too.

Acknowledgment

The work was supported by a Grant-in-Aid for Scientific Research (B) (17370055) (to S.I.) and by the 21st Century Center of Excellence program titled “the origin of the universe and matter” (G11) from the Ministry of Education, Science, Sports and Culture (to S.I. and T.T.). The authors thank Dr. N. Wakao, Iwate Univ., for his kind gift of *A. rubrum* cells.

References

[1] N. Wakao, N. Yokoi, N. Isoyama, A. Hiraishi, K. Shimada, M. Kobayashi, H. Kise, M. Iwaki, S. Itoh, S. Takaichi, Y. Sakurai, Discovery of natural photosynthesis using Zn-containing bacteriochlorophyll in an aerobic bacterium *Acidiphilium rubrum*, Plant Cell Physiol. 37 (1996) 889–893.

[2] S. Takaichi, N. Wakao, A. Hiraishi, S. Itoh, K. Shimada, Nomenclature of metal-substituted (bacterio) chlorophylls in natural photosynthesis: Metal-(bacterio)chlorophyll and M-(B)Chl, Photosynth. Res. 59 (1999) 255–256.
[3] K. Shimada, S. Itoh, M. Iwaki, K.V.P. Nagashima, K. Matsuura, M. Kobayashi, N. Wakao, in: G. Garab (Ed.), Reaction center complex based on Zn-bacteriochlorophyll from *Acidiphilium rubrum*, Photosynthesis: Mechanisms and Effects, vol. II, Kluwer Academic Publishers, Dordrecht, 1998, pp. 909–912.
[4] N. Wakao, A. Hiraishi, K. Shimada, M. Kobayashi, S. Takaichi, M. Iwaki, S. Itoh, Discovery, characteristics, and distribution of zinc-BChl in aerobic acidophilic bacteria including *Acidiphilium* species and other related acidophilic bacteria, in: G.A. Peschek, W. Loffelhardt, G. Schmetterer (Eds.), The phototrophic Prokaryotes, Kluwer Academic Publishers, New York, 1999, pp. 745–750.
[5] A. Hiraishi, K. Shimada, Aerobic anoxygenic photosynthetic bacteria with zinc-bacteriochlorophyll, J. Gen. Appl. Microbiol. 47 (2001) 161–180.
[6] P.L. Wichlacz, R.F. Unz, T.A. Langworthy, *Acidiphilium angustum* sp. nov., *Acidiphilium facilis* sp. nov., and *Acidiphilium rubrum* sp. nov.: acidophilic heterotrophic bacteria isolated from acidic coal mine drainage, Int. J. Syst. Bacteriol. 36 (1986) 197–201.
[7] N. Wakao, T. Shiba, A. Hiraishi, M. Ito, Y. Sakurai, Distribution of bacteriochlorophyll *a* in species of the genus *Acidiphilium*, Curr. Microbiol. 27 (1993) 277–279.
[8] N. Kishimoto, F. Fukaya, K. Inagaki, T. Sugio, H. Tanaka, T. Tano, Distribution of bacteriochlorophyll *a* among aerobic and acidophilic bacteria and light-enhanced CO_2-incorporation in *Acidiphilium rubrum*, FEMS Microbiol. Ecol. 16 (1995) 291–296.
[9] J.F. Imhoff, A. Hiraishi, Aerobic bacteria containing bacteriochlorophyll and belonging to the alphaproteobacteria, in: D.J. Brenner, N.R. Krieg, J.T. Staley, G.M. Garrity (Eds.), Bergey's manual of systematic bacteriology, 2nd ed., The proteobacteria part A introductory essays, vol. 2, Springer-Verlag, New York, 2005, pp. 133–136.
[10] M. Akiyama, M. Miyake, H. Kise, M. Narato, N. Wakao, K. Inoue, M. Kobayashi, Accumulation of poly-β-hydroxybutyrate in an acidophilic photosynthetic purple bacterium *Acidiphilium rubrum*, Photomed. Photobiol. 21 (1999) 101–104.
[11] Y. Matsuzawa, T. Kanbe, J. Suzuki, A. Hiraishi, Ultrastructure of the acidophilic aerobic photosynthetic bacterium *Acidiphilium rubrum*, Curr. Microbiol. 40 (2000) 398–401.
[12] S. Itoh, M. Iwaki, N. Wakao, K. Yoshizu, A. Aoki, K. Tazaki, Accumulation of Fe, Cr and Ni metals inside cells of acidophilic bacterium *Acidiphilium rubrum* that produces Zn-containing bacteriochlorophyll *a*, Plant Cell Physiol. 39 (1998) 740–744.
[13] A. Hiraishi, K.V.P. Nagashima, K. Matsuura, K. Shimada, S. Takaichi, N. Wakao, Y. Katayama, Phylogeny and photosynthetic features of *Thiobacillus acidophilus* and related acidophilic bacteria: its transfer to the genus *Acidiphilium* as *Acidiphilium acidophilum* comb. nov., Int. J. Syst. Bacteriol. 48 (1998) 1389–1398.
[14] A. Hiraishi, Y. Matsuzawa, T. Kanbe, N. Wakao, *Acidisphaera rubrifaciens* gen. nov., sp. nov., an aerobic bacteriochlorophyll-containing bacterium isolated from acidic environments, Int. J. Syst. Evol. Microbiol. 50 (2000) 1539–1546.
[15] T. Masuda, K. Inoue, M. Masuda, M. Nagayama, A. Tamaki, H. Ohta, H. Shimada, K. Takamiya, Magnesium insertion by magnesium chelatase in the biosynthesis of zinc bacteriochlorophyll *a* in an aerobic acidophilic bacterium *Acidiphilium rubrum*, J. Biol. Chem. 274 (1999) 33594–33600.
[16] I. Ikegami, A. Nemoto, K. Sakashita, The formation of Zn-Chl *a* in *Chlorella* heterotrophically grown in the dark with an excessive amount of Zn^{2+}, Plant Cell Physiol. 46 (2005) 729–735.
[17] T.A. Evans, J.J. Katz, Evidence for 5- and 6-coordinated magnesium in bacteriochlorophyll *a* from visible absorption spectroscopy, Biochim. Biophys. Acta 396 (1975) 414–426.
[18] W.R. Scheidt, M.E. Kastner, K. Hatano, Stereochemistry of the toluene solvate of α, β, γ, δ-tetraphenylporphinatozinc (II), Inorg. Chem. 17 (1978) 706–710.
[19] H. Tamiaki, M. Amakawa, Y. Shimono, R. Tanikaga, A.R. Holzwarth, K. Schaffner, Synthetic zinc and magnesium chlorin aggregates as models for supramolecular antenna complexes in chlorosomes of green photosynthetic bacteria, Photochem. Photobiol. 63 (1996) 92–99.
[20] M. Kobayashi, M. Akiyama, M. Yamamura, H. Kise, N. Wakao, N. Ishida, M. Koizumi, H. Kano, T. Watanabe, Comparison of physicochemical properties of metallobacteriochlorophylls and metallochlorophylls, Z. Phys. Chem. 213 (1999) 207–214.
[21] T. Watanabe, A. Nakamura, M. Kobayashi, Chemical analytical approach to the molecular machinery of photosynthesis—quest for exotic chlorophylls in the reaction centers, Chem. Soc. Japan 2 (2002) 117–128.
[22] Y. Takeuchi, Y. Amao, Light-harvesting properties of zinc complex of chlorophyll-*a* from *spirulina* in surfactant micellar media, BioMetals 18 (2005) 15–21.
[23] F. Li, S. Gentemann, W.A. Kalsbeck, J. Seth, J.S. Lindsey, D. Holten, D.F. Bocian, Effects of central metal ion (Mg, Zn) and solvent on singlet excited-state energy flow in porphyrin-based nanostructures, J. Mater. Chem. 7 (1997) 1245–1262.
[24] J. Fiedor, L. Fiedor, N. Kammhuber, A. Scherz, H. Scheer, Photodynamics of the bacteriochlorophyll-carotenoid system. 2. Influence of central metal, solvent and β-carotene on photobleaching of bacteriochlorophyll derivatives, Photochem. Photobiol. 76 (2002) 145–152.
[25] M. Kobayashi, M. Yamamura, M. Akiyama, H. Kise, K. Inoue, M. Hara, N. Wakao, K. Yahara, T. Watanabe, Acid resistance of Zn-bacteriochlorophyll *a* from an acidophilic bacterium *Acidiphilium rubrum*, Anal. Sci. 14 (1998) 1149–1152.
[26] M. Mimuro, M. Kobayashi, K. Shimada, K. Uezono, T. Nozawa, Magnetic circular dichroism properties of reaction center complexes isolated from the zinc-bacteriochlorophyll *a*-containing purple bacterium *Acidiphilium rubrum*, Biochemistry 39 (2000) 4020–4027.
[27] K.V.P. Nagashima, K. Matsuura, N. Wakao, A. Hiraishi, K. Shimada, Nucleotide sequences of genes coding for photosynthetic reaction centers and light-harvesting proteins of *Acidiphilium rubrum* and related aerobic acidophilic bacteria, Plant Cell Physiol. 38 (1997) 1249–1258.
[28] V. Sundström, R.V. Grondelle, H. Bergström, E. Åkesson, T. Gillbro, Excitation-energy transport in the bacteriochlorophyll antenna systems of *Rhodospirillum rubrum* and *Rhodobacter sphaeroides*, studied by low-intensity picosecond absorption spectroscopy, Biochim. Biophys. Acta 851 (1986) 431–446.
[29] R.V. Grondelle, H. Bergström, V. Sundström, T. Gillbro, Energy transfer within the bacteriochlorophyll antenna of purple bacteria at 77 K, studied by picosecond absorption recovery, Biochim. Biophys. Acta 894 (1987) 313–326.
[30] A. Freiberg, 19. Coupling of antennas to reaction centers, in: R.E. Blankenship, M.T. Madigan, C.E. Bauer (Eds.), Anoxygenic Photosynthetic Bacteria, Kluwer Academic Publishers, Dordrecht, 1995, pp. 385–398.
[31] C. Kirmaier, D. Holten, in: J. Deisenhofer, J.R. Norris (Eds.), 3. Electron transfer and charge recombination reactions in wild-type and mutant bacterial reaction centers, The photosynthetic reaction center, vol. II, Academic Press, San Diego, 1993, pp. 49–70.
[32] N.W. Woodbury, J.P. Allen, 24. The pathway, kinetics and thermodynamics of electron transfer in wild type and mutant reaction centers of purple nonsulfur bacteria, in: R.E. Blankenship, M.T. Madigan, C.E. Bauer (Eds.), Anoxygenic Photosynthetic Bacteria, Kluwer Academic Publishers, Dordrecht, 1995, pp. 527–557.
[33] R.J. Stanley, B. King, S.G. Boxer, Excited state energy transfer pathways in photosynthetic reaction centers. 1. Structural symmetry effects, J. Phys. Chem. 100 (1996) 12052–12059.
[34] J. Deisenhofer, O. Epp, I. Sinning, H. Michel, Crystallographic refinement at 2.3 Å resolution and refined model of the photosynthetic reaction centre from *Rhodopseudomonas viridis*, J. Mol. Biol. 246 (1995) 429–457.
[35] K. Matsuura, K. Shimada, Cytochromes functionally associated to photochemical reaction centers in *Rhodopseudomonas palustris* and *Rhodopseudomonas acidophila*, Biochim. Biophys. Acta 852 (1986) 9–18.
[36] R.J. Cogdell, T.G. Monger, W.W. Parson, Carotenoid triplet states in reaction centers from *Rhodopseudomonas sphaeroides* and *Rhodospirillum rubrum*, Biochim. Biophys. Acta 408 (1975) 189–199.
[37] H. Chosrowjan, N. Mataga, N. Nakashima, Y. Imamoto, F. Tokunaga, Femtosecond–picosecond fluorescence studies on excited state dynamics

of photoactive yellow protein from *Ectothiorhodospira halophila*, Chem. Phys. Lett. 270 (1997) 267–272.
[38] P.L. Dutton, Redox potentiometry: determination of midpoint potentials of oxidation–reduction components of biological electron-transfer systems, Methods Enzymol. 54 (1978) 411–435.
[39] E.M. Franken, A.Y. Shkuropatov, C. Francke, S. Neerken, P. Gast, V.A. Shuvalov, A.J. Hoff, T.J. Aartsma, Reaction centers of *Rhodobacter sphaeroides* R-26 with selective replacement of bacteriopheophytin by pheophytin *a* I. Characterisation of steady-state absorbance and circular dichroism, and of the $P^{+}Q_{A}^{-}$ state, Biochim. Biophys. Acta 1319 (1997) 242–250.
[40] D.M. Jonas, M.J. Lang, Y. Nagasawa, T. Joo, G.R. Fleming, Pump-probe polarization anisotropy study of femtosecond energy transfer within the photosynthetic reaction center of *Rhodobacter sphaeroides* R26, J. Phys. Chem. 100 (1996) 12660–12673.
[41] B.A. King, T.B. McAnaney, A. deWinter, S.G. Boxer, Excited state energy transfer pathways in photosynthetic reaction centers. 3. Ultrafast emission from the monomeric bacteriochlorophylls, J. Phys. Chem., B 104 (2000) 8895–8902.
[42] P.L. Dutton, J.B. Jackson, Thermodynamic and kinetic characterization of electron-transfer components *in situ* in *Rhodopseudomonas spheroides* and *Rhodospirillum rubrum*, Eur. J. Biochem. 30 (1972) 495–510.
[43] J.B. Jackson, P.L. Dutton, The kinetic and redox potentiometric resolution of the carotenoid shifts in *Rhodopseudomonas spheroides* chromatophores: their relationship to electric field alterations in electron transport and energy coupling, Biochim. Biophys. Acta 325 (1973) 102–113.
[44] J.C. Williams, R.G. Alden, H.A. Murchison, J.M. Peloquin, N.W. Woodbury, J.P. Allen, Effects of mutations near the bacteriochlorophylls in reaction centers from *Rhodobacter sphaeroides*, Biochemistry 31 (1992) 11029–11037.
[45] V. Nagarajan, W.W. Parson, D. Davis, C.C. Schenck, Kinetics and free energy gaps of electron-transfer reactions in *Rhodobacter sphaeroides* reaction centers, Biochemistry 32 (1993) 12324–12336.
[46] X. Lin, H.A. Murchison, V. Nagarajan, W.W. Parson, J.P. Allen, J.C. Williams, Specific alteration of the oxidation potential of the electron donor in reaction centers from *Rhodobacter sphaeroides*, Proc. Natl. Acad. Sci. U. S. A. 91 (1994) 10265–10269.
[47] A. Ivancich, M. Kobayashi, F. Drepper, I. Fathir, T. Saito, T. Nozawa, T.A. Mattioli, Hydrogen-bond interactions of the primary donor of the photosynthetic purple sulfur bacterium *Chromatium tepidum*, Biochemistry 35 (1996) 10529–10538.
[48] R.A. Goldstein, L. Takiff, S.G. Boxer, Energetics of initial charge separation in bacterial photosynthesis: the triplet decay rate in very high magnetic fields, Biochim. Biophys. Acta 934 (1988) 253–263.
[49] A. Ogrodnik, M. Volk, R. Letterer, R. Feick, M.E. Michel-Beyerle, Determination of free energies in reaction centers of *Rb. sphaeroides*, Biochim. Biophys. Acta 936 (1988) 361–371.
[50] L. Takiff, S.G. Boxer, Phosphorescence from the primary electron donor in *Rhodobacter sphaeroides* and *Rhodopseudomonas viridis* reaction centers, Biochim. Biophys. Acta 932 (1988) 325–334.
[51] N.W.T. Woodbury, W.W. Parson, Nanosecond fluorescence from isolated photosynthetic reaction centers of *Rhodopseudomonas sphaeroides*, Biochim. Biophys. Acta 767 (1984) 345–361.
[52] N.W. Woodbury, W.W. Parson, M.R. Gunner, R.C. Prince, P.L. Dutton, Radical-pair energetics and decay mechanisms in reaction centers containing anthraquinones, naphthoquinones or benzoquinones in place of ubiquinone, Biochim. Biophys. Acta 851 (1986) 6–22.
[53] C. Geskes, G. Hartwich, H. Scheer, W. Mantele, J. Heinze, An electrochemical and spectroelectrochemical investigation of metal-substituted bacteriochlorophyll *a*, J. Am. Chem. Soc. 117 (1995) 7776–7783.
[54] H. Scheer, G. Hartwich, Bacterial reaction centers with modified tetrapyrrole chromophores, in: R.E. Blankenship, M.T. Madigan, C.E. Bauer (Eds.), Anoxygenic photosynthetic bacteria, Kluwer Academic Publishers, Dordrecht, 1995, pp. 649–663.
[55] M. Kobayashi, A. Takaya, N. Kanai, Y. Ota, T. Saito, Z.Y. Wang, T. Nozawa, Reconstitution and replacement of bacteriochlorophyll *a* molecules in photosynthetic reaction centers, J. Biochem. 136 (2004) 363–369.
[56] X.J. Jordanides, G.D. Scholes, G.R. Fleming, The mechanism of energy transfer in the bacterial photosynthetic reaction center, J. Phys. Chem. B 105 (2001) 1652–1669.
[57] M. Du, S.J. Rosenthal, X. Xie, T.J. DiMagno, M. Schmidt, D.K. Hanson, M. Schiffer, J.R. Norris, G.R. Fleming, Femtosecond spontaneous-emission studies of reaction centers from photosynthetic bacteria, Proc. Natl. Acad. Sci. U. S. A. 89 (1992) 8517–8521.
[58] R.A. Marcus, On the theory of oxidation–reduction reactions involving electron transfer, J. Chem. Phys. 24 (1956) 966–978.
[59] A.L.M. Haffa, S. Lin, E. Katilius, J.C. Williams, A.K.W. Taguchi, J.P. Allen, N.W. Woodbury, The dependence of the initial electron-transfer rate on driving force in *Rhodobacter sphaeroides* reaction centers, J. Phys. Chem. B 106 (2002) 7376–7384.